A facile one-step hydrothermal preparation of $Mn(VO_3)_2$ under different pH conditions and their photocatalytic performance

Jinqiu Huang,[a] Ruijie Liang,[a] Yuan Huang[a], Feng Li[a, b], Taohai Li[*a, b]

[a]*College of Chemistry, Key Laboratory of Environment-Friendly Chemistry and Applications Ministry of Education, Xiangtan University, Xiangtan.411105,China.*

[b] *Nano and Molecular Systems Research Unit, Faculty of Science, P. O. Box 3000, University of Oulu, FIN-90014, Finland*

ABSTRACT

Adopting $MnSO_4 \cdot H_2O$ and $K_6V_{10}O_{28} \cdot 9H_2O$ as the manganese and vanadium source, respectively, the $Mn(VO_3)_2$ product was obtained by the facile one-step hydrothermal method under different pH conditions without adding any additives. The effects of pH on microstructure and photoactivity were investigated. The photocatalytic results demonstrate that $Mn(VO_3)_2$ prepared at pH = 5.0 showed optimal photoactivity in the photodegradation of RhB under UV light irradiation，and 95% of RhB was degraded by irradiation within 80 minutes, offering a new insight with the functional materials in the application of the photochemistry field.

Keywords: $Mn(VO_3)_2$; Microstructure; Hydrothermal; XPS; Photocatalytic

* Correspondence Author. Tel.: +86-731-58292202; fax: +86-731-8292251;

E-mail address:hnlth@xtu.edu.cn

1.Introduction

The increasing pollution of water by industrial wastes demands effective solution methods of modern decontamination technology urgently, where photocatalytic degradation of harmful organic matters with semiconductor catalysts has been considered as a novel and efficient route [1]. Among various synthetic semicoductors, the group of metal vanadate has shown multifunctional potentials as photocatalysts in water purification [2-5]. However, the species of metal metavanadates are mainly limited to the $AgVO_3$, $Cu(VO_3)_2$ and their composites [6-10]. The $Mn(VO_3)_2$ (manganese metavanadate) receives much less attentions than its possible applications, though it has been referred to a promising electrode material in the Li-ion battery [11-12]. It has been general noticed the performances of catalytic activities heavily depend on the morphologies of catalysts, which are subjected to the preparation conditions. Hence, the synthesis of $Mn(VO_3)_2$ with the controlled crystal form and morphology is highly desirable.

Up to now, only a few preparation of $Mn(VO_3)_2$ have been reported. For example, $Mn(VO_3)_2 \cdot yH_2O$ compounds were synthesized with a precipitation method [13-14] or refluxing route with the mixture of V_2O_5 with $Mn(CH_3COO)_2$ in water medium [15]. The powder form of $Mn(VO_3)_2$ can also be reached via route-rheological phase reaction method or polymer gellation method [16-17]. However, the preparation conditions are complicated, and the purity of the synthetic product is hardly controlled precisely. Hydrothermal method has also been employed

in preparations of manganese metavanadate with other crystal forms and morphologies. [18-21] Through this method, morphologies of the final products can be easily controlled by changing reaction conditions, like pH value, temperature, reaction time and reagent concentration. In this paper, a facile one-step hydrothermal method of monoclinic $Mn(VO_3)_2$ was reported. Different morphologies of $Mn(VO_3)_2$ were obtained easily by tuning the reaction pH without any additives. In this paper, $K_6V_{10}O_{28}\cdot 9H_2O$ was employed as the vanadium source instead of the conventional NH_4VO_3 or V_2O_5 source adopted in most prior studies. It's the first time that the $Mn(VO_3)_2$ was employed as a photocatalyst to degrade RhB aqueous solution under the UV irradiation achieving good results.

2. Experimental

2.1 Material and synthesis

The $K_6V_{10}O_{28}\cdot 9H_2O$ was employed as the vanadium source. It was prepared by a route as shown in the literature[22]. $MnSO_4\cdot H_2O$ was purchased from Shan-tou Xilong Chemical Factory. All of the chemical reagents were of analytical purity and used without further purification.

In a typical synthetic procedure, $K_6V_{10}O_{28}\cdot 9H_2O$ (0.65 g) and $MnSO_4\cdot H_2O$ (0.85 g) were dissolved into the distilled water (20 mL) with stirring at room temperature. After stirring for 30 min, the pH value of the final suspension was adjusted to 3.0, 5.0, 7.0, 9.0, 11.0 respectively by dropping 1M NaOH or H_2SO_4 solutions. Finally, the suspension was transferred into stainless steel autoclaves lined with 25 mL PTFE

and heated up to 180℃ for 24 h. After naturally cooling down to room temperature, the precipitates were washed alternately by distilled water and absolute ethanol for several times, and then dried in vacuum at about 70℃ for 20 h.

2.2 Characterizations

The products were examined by XRD (MiniFlex II) using Cu Kα radiation (λ = 0.15406 nm) from 10 to 60 of 2teta angle. Morphological determinations were performed on a JSM-6610LV Scanning Electron Microscope (SEM) and a FEI Tecnai G20 transmission electron microscope (TEM). A Perkin-Elmer PHI 5000C spectrometer was employed to record X-ray photoelectron spectra (XPS) using a monochromatized Al Kα excitation as the incident source. The UV-visible absorption spectra were recorded on a Lambda 25 UV-vis spectrophotometer (Perkin-Elmer, USA) in the range of 300-800 nm.

2.3 Dye adsorption measurements

Rhodamine B (RhB) was chosen as the model organic pollutant to assess the photocatalytic activities of the prepared samples. A solution containing 100 mL of 0.010 g / L RhB and 0.10 g of $Mn(VO_3)_2$ powders was magnetically stirred in a light-free environment for 30 minutes. As shown in Figure S1 in Supporting Information, the suspension has reached to the adsorption-desorption equilibrium of RhB on the catalyst surfaces after magnetically stirred 30 min in the dark. And then catalyzed under UV light. In the experimental setup, a 500 W Hg lamp (λ < 420 nm) was employed as the light source. During this process, the mixture was placed in a

photoreactor and magnetically stirred, and the circulating water was turned on to maintain the temperature of the suspension in the range of 22-28°C. At intervals of 30 minutes, about 5 mL of the suspension was taken out and centrifuged, and then the photocatalyst particles were removed by centrifugation. The RhB solution was analyzed using a UV-visible spectrophotometer (λ25 spectrometer) and observed a maximum absorbance at 665 nm.

3.Results and discussion

The microstructures of the $Mn(VO_3)_2$ samples produced from the reactions with different pH values were researched with SEM and TEM test. As shown in Figure 1, the morphologies of the $Mn(VO_3)_2$ samples rely on the pH of the reactant mixture, and all the products show irregular shapes. When the pH value is 9.0 during the synthesis, the products are large rod or bulk aggregate with the sizes ranging from 20 μm-40 μm (Figure 1a). When the pH value is 7.0, the product is composed of large number of irregular lumps or strips with the size about 2 μm. When the pH value decreased to 5.0, the size of $Mn(VO_3)_2$ samples becomes relatively small. As the pH value declines to 3.0, the $Mn(VO_3)_2$ product eventually turned into a large number of irregular long strips. The size of long strips is smaller than that of $Mn(VO_3)_2$ samples produced at pH = 5.0. This is because the growth mechanism of the product is different under different pH conditions. Therefore, it can be seen that it is more favorable to form $Mn(VO_3)_2$ with smaller size under neutral and acidic conditions. in

As shown in the TEM image of Figure 1e, the size of the nanorods is about 1 μm and 100-200 nm in the longitudinal and transverse direction, respectively.

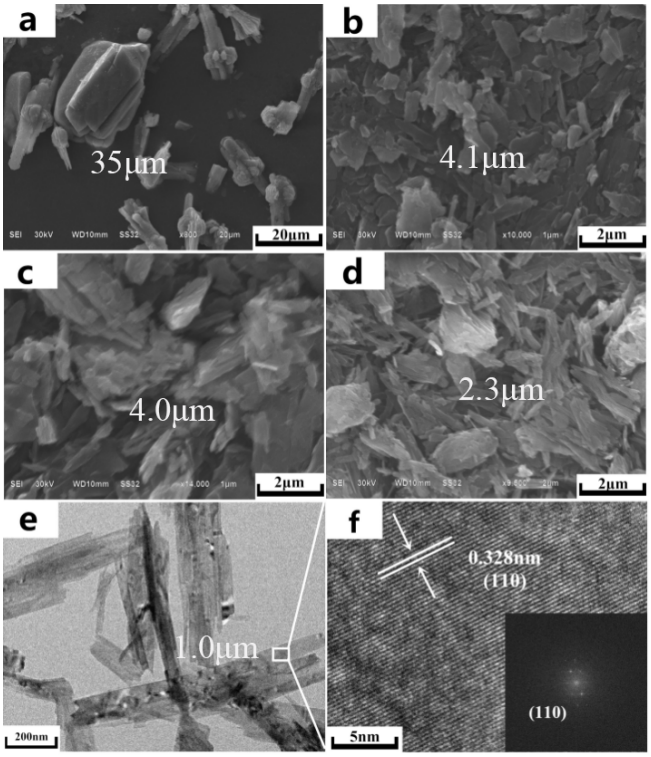

Figure 1. SEM images of $Mn(VO_3)_2$ with different pH values: (a) pH = 9.0, (b) pH = 7.0, (c) pH = 5.0, (d) pH = 3.0. The TEM images of $Mn(VO_3)_2$ at pH = 3.0: (e) low, (f) high-resolution and FFT inset.

Morphological determinations show that the acidity and alkalinity have an important influence on the nucleation and crystallization of the products. In the acidic environment, precursors are more prone to rapid nucleation and form a large number of irregular strip products with smaller size. In the alkaline environment, the nucleation is inhibited, and the product is more inclined to crystallize and form large irregular blocks. The phenomenon can be explained by the fact that the variation of

pH could affect the solubility of $MnSO_4$ and re-crystallization of $Mn(VO_3)_2$. The solubility of $MnSO_4$ increased with the decreasing of pH when pH < 7.0 [23]. A higher solubility of $MnSO_4$ provides a higher concentration of Mn^{2+} ions for the precipitation of $Mn(VO_3)_2$, promoting the nucleation of $Mn(VO_3)_2$. In the alkaline condition (pH = 9.0), the hydroxyl groups bonded on the surface of the $MnSO_4$ crystals may inhibit the dissolution process of Mn^{2+} ions into the solution, which kinetically delay the formation of $Mn(VO_3)_2$. The HRTEM and FFT results (Figure 1f) show that the interplane spacing of the $Mn(VO_3)_2$ products is 0.328nm, exactly corresponding to the crystal plane (110) of monoclinic $Mn(VO_3)_2$.

Figure 2 depicts the XRD atlas of the as-synthesized specimens. The XRD atlas for products synthesized at the pH values from 3.0 to 7.0 are well indexed to standard values for the $Mn(VO_3)_2$ (JCPDS No. 35-0139, a = 9.315, b = 3.536, c = 6.754). The impurity peak at 2θ = 44.346° when the pH = 3.0 and 7.0 is attributed to the existence of crystalline water in the product, corresponding to the (6 0 0) plane of $MnV_2O_6{\cdot}4H_2O$ (PDF#49-1012). When pH is 9.0, the phase of the product was no longer $Mn(VO_3)_2$, but turned to the monoclinic phase of $Mn_2V_2O_7$ (PDF#38-0034). The impurity peak at 2θ = 44.346° is also due to the presence of crystal water in the product. In the low H^+ alkaline conditions, the $V_{10}O_{28}^{6-}$ underwent proton dissociated and transferred to $V_2O_7^{4-}$. The $V_2O_7^{4-}$ in the solution reacted with Mn^{2+}, yielding the $Mn_2V_2O_7$. In a word, the acidity and alkalinity of solution play an important role in the formation of crystallinity, affecting the type of crystal. The pure $Mn(VO_3)_2$ could

be obtained only in the weak acid environment.

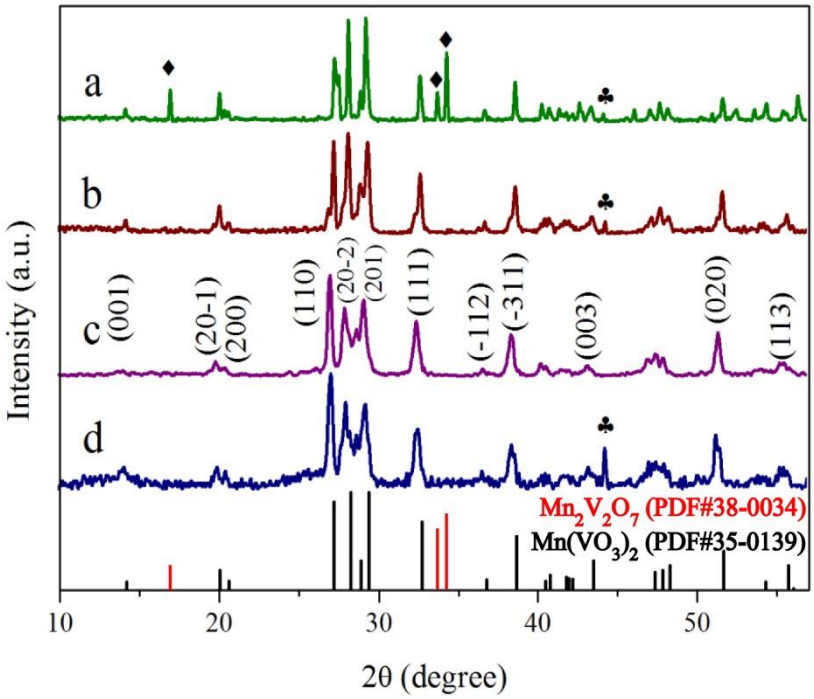

Figure 2. XRD atlas of specimens obtained at (a) pH = 9.0, (b) pH = 7.0, (c) pH = 5.0, (d) pH = 3.0.

To further elucidate the chemical states of the product, the sample prepared at pH = 3.0 was selected as the model of XPS analysis. The general survey (Figure 3 a) demonstrates the presence of Mn, V, and O. As shown in the Figure 3, there is a carbon peak which comes from the instrument. The C1s is employed in the energy calibration. In the high-resolution XPS s of Mn2p (Figure. 2b), two intense peaks were found at 641.8eV and 652.9 eV, attributed to the 2p3/2 and 2p1/2 of the Mn ions. A satellite peak at 647eV is attributed to the ligand-to-metal charge transfer shake-up process [24-25]. The above results prove that the primary chemical state of the Mn is +2. In Figure 3c, the characteristic peaks of V were observed at 524.9eV and 517.3 eV,

corresponding to V2p1/2 and V2p3/2 from the V^{5+} ions respectively [19]. The O1s peaks at 530.2eV is attributed to the coordination of oxygen in V–O. [26] The results of XPS analysis are accordance with the result of XRD analysis, and further confirm the existence of $Mn(VO_3)_2$.

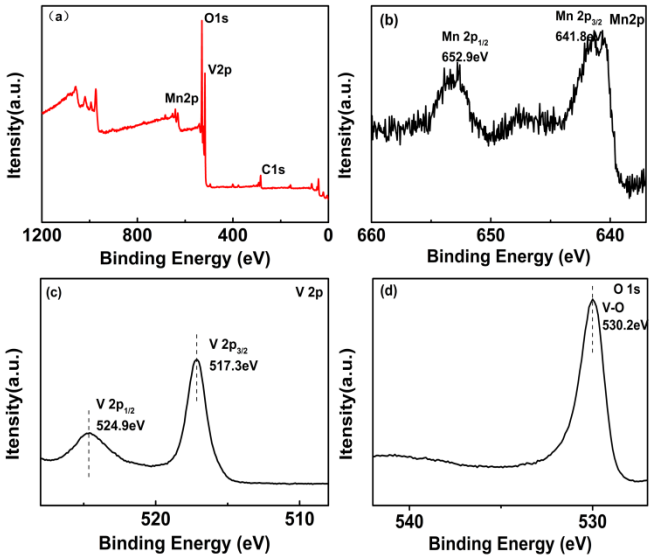

Figure 3. The XPS spectra of the $Mn(VO_3)_2$ synthesized at pH = 3.0 . (a) the entire spectra e, (b) Mn2p, (c) V2p, (d) O1s.

Photocatalytic activity of our samples was studied by the ultraviolet light degradation of RhB. Figure 4 (a) shows the concentration variation of RhB aqueous solution with reaction time. The negative value on the horizontal axis represents 30 minutes of adsorption, and 0 minutes represents the beginning of degradation. The blank test showed that the self-catalysis of RhB under light could almost be neglected. Then 120 min of UV light irradiation, the photodegradation efficiencies of RhB are 75%, 100%, 88.5% and 20.2% for samples prepared at pH = 3.0, pH = 5.0, pH = 7.0 and pH = 9.0, respectively. Apparently, the sample from the reaction with pH of 5.0

showed the best photocatalytic activity among all samples, and 95% of RhB was degraded by irradiation within 80 minutes. Figure 4 (b) shows the UV-visibie absorption spectra of RhB solution after $Mn(VO_3)_2$ treatment at pH of 5.0. The characteristic UV-vis absorption peak of the RhB solution is located at 545nm. With the increasing of light irradiation time, the maximum absorption peak intensity of the RhB solution at 545nm decreases significantly. When the light irradiation time increases to 100 minutes, the concentration of the RhB solution decreases to 0 mg·L, and the color of the RhB solution changes from rose red to colorless. This is probably due to the higher purity of the sample yielding the efficient catalytic efficiency.

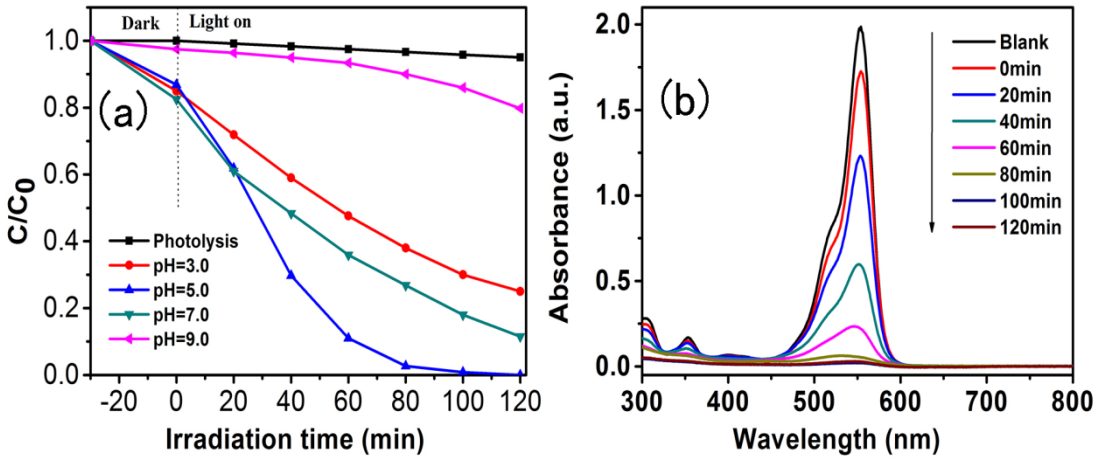

Figure 4. (a) C/C_0 of RhB with time in the presence of $Mn(VO_3)_2$; (b) UV-visibie absorption spectra of RhB solution after $Mn(VO_3)_2$ treatment at pH=5.0.

4. Conclusion

In summary, the monoclinic $Mn(VO_3)_2$ have been prepared from $K_6V_{10}O_{28}\cdot 9H_2O$ by a simple one-step hydrothermal method. The microstructure of the product could be controlled by changing the pH of reaction mixture. The photocatalytic results

demonstrate that $Mn(VO_3)_2$ product prepared at pH of 5.0 shows the optimal photoactivity for the photodegradation of RhB under UV light irradiation. This research is supposed to provide a neoteric insight with the control synthesis of $Mn(VO_3)_2$ and application in the field of photocatalysis.

Acknowledgements

The authors acknowledge with thanks the financial support of the National Natural Science Foundation of China (21601149) and Hunan 2011 Collaborative Innovation Center of Chemical Engineering & Technology with Environmental Benignity and Effective Resource Utilization. Feng Li thanks the support of China Scholarship Council.

References

[1] H. Kisch, Angew. Chem. Int. Ed. 52 (2013) 812–847.

[2] M. Y. Ye, Z.H. Zhao, Z.F. Hu, et al. Angew. Chem. Int. Edit. 56 (2017) 8407.

[3] T.W. Kim, K. S. Choi, Science. 343 (2014) 990.

[4] J. Ye, Z. Zou, M. Oshikiri, A. Matsushita, M. Shimoda, et. al. Chem. Phys. Lett. 356 (2002) 221.

[5] R. G. Li, F. X. Zhang, D. G. Wang, J. X. Yang, M. R. Li, et. al. Nat. Commun. 4 (2013) 1432.

[6] V. Sivakumar, R. Suresh, K. Giribabu, V. Narayanan, et al., Solid State Sci. 39 (2014) 34-39.

[7] X. Qiao, Y. Wan, Y. Li, L. Qin, H. J. Seo, et al., Appl. Surf. Sci. 368 (2016) 63-68.

[8]Y. Sang, L. Kuai, C. Y. Chen, Z. Fang, et al., ACS Appl. Mat. Interfaces, 6 (2014) 5061-5068.

[9] M. Harb, D. Masih, K. Takanabe, Phys. Chem. Chem. Phys. 16 (2014) 18198-18204.

[10] J. Xu, C.G.Hu, Y. Xi, B. Y. Wan, C. L. Zhang, et al. Solid State Sci. 14 (2012) 535–539.

[11] Y. Piffard, F. Leroux, D. Guyomard, et al. J. Power Sources. 68 (1997) 698-703.

[12] F. Leroux, Y. Piffard, G. Ourvard, et al, Chem Mater. 11 (1999) 2948-2959.

[13] E. Andrukaitis, J. Power Sources. 68 (1997) 652-655.

[14] E. Andrukaitis, G. L. Torlone, and I. R. Hill, J. Power Sources. 81 (1999) 651-655.

[15] T. Morishita, K. Nomura, T. Inamasu, M. Inagaki, Solid State Ionics. 176 (2005) 2235-2241.

[16] L. Tan, H. W. Liu, Inorg. Mater. 46 (2010) 201-205.

[17] S. S. Kim, H. Ikuta, M. Wakihara, Solid State Ionics. 139 (2001) 57-65.

[18] M. Inagaki, T. Morishita, M. Hirano, et al., Solid State Ionics. 156 (2003) 275-282.

[19] Y. Liu, Y. G. Zhang, J. Du, W. C. Yu, Y. T. Qian, J. Cryst. Growth. 133 (2005) 117-120.

[20] W. Huang, S. Gao, X. Ding, L. L. Jiang, M. D. Wei, J. Alloys Compd. 41 (2010) 185-188.

[21] S. J. Lei, K. B. Tang, Y. Jin, C. H. Chen, Nanotechnology. 18 (2007) 751-753.

[22]Xu J N, Yang G Y, Sun H R, et al. Chemical Research and Application. 9 (1997) 576-581.

[23]Li F, Liu J, Yang G, et al. Journal of Crystal Growth. 374 (2013) 31-36.

[24]A.P. Grosvenor, E. M. Bellhouse, A. Korinek, et al. Appl. Surf. Sci. 379 (2016) 242-248.

[25] M.C. Biesinger, B.P. Payne, A.P. Grosvenor, et al. Appl. Surf. Sci. 357 (2011) 2717-2730.

[26] C.Y. Yang, F. Li, T.H. Li. CrystEngComm. 17 (2015) 7676-7683.